Anharmonic contribution to the temperature dependence of photoemission core-level spectroscopy of adsorbates on surfaces: Oxygen on Rh(110)

Alessandro Baraldi, Silvano Lizzit, Daniele Cocco, and Giorgio Paolucci

Sincrotrone Trieste S.C.p.A., S.S. 14 Km 163.5, 34012 Trieste, Italy

(Received 3 October 1997)

High-resolution x-ray photoelectron spectroscopy has been used to investigate the temperature behavior of the O $1s$ and O $2s$ core-level photoemission signals from the O-$(2\times2)p2mg$ structure on Rh(110). With increasing temperature we observe a continuous shift of the photoemission peaks to lower binding energy. The width of the peaks increases with increasing temperature, as previously reported for other systems. Since the adsorption site of the O atoms is independent of temperature, the phenomenon is interpreted as due to anharmonic contributions to the potential-energy curve. [S0163-1829(98)04804-8]

Core-level photoemission, also known as x-ray photoemission spectroscopy (XPS) is a widely used technique to study adsorbed atoms and molecules on surfaces.[1,2] It is possible to identify the nature and the coverage of adsorbed species, and the binding-energy shifts of the core levels can be used to understand the chemical and geometrical state of atoms and molecules present on the surface.

In this field the temperature dependence of the photoemission line shape has been the subject of a number of studies in the last ten years, but most of the work has been done on clean metal surfaces,[3–7] while a limited number of experiments have been performed on chemisorption systems.[8–13] The reason for this is that until recently a high-resolution XPS spectrum of an adsorbate core level required several minutes to be acquired, because of the low-photon intensity of conventional laboratory x-ray sources or second generation synchrotron light sources and low concentration of photoemitters. The data acquisition time must be limited because small amounts of contamination of the adsorbed layers by the residual gas, even in ultrahigh-vacuum conditions ($\sim10^{-8}$ Pa), can give rise to changes of photoemission line shapes.

In order to interpret the photoemission results from molecules and atoms, a model based on vibrational effects was introduced by Nilsson and Mårtensson in the late 1980s.[9] They assume that, since the photoionization process is much faster than the geometrical relaxation of the atoms, the final state of the photoionized atom or molecule preserves the same geometry of the state before ionization. However, the equilibrium atomic position and the forces between atoms are different in the ionized and in the neutral state. As predicted by the Franck-Condon transition principle the initial-state vibrational wave function is projected on the final-state potential-energy curve and transitions to different vibrational states are created. Experimental evidence of this is the observed broadening in the core-level spectra of carbon, nitrogen, and oxygen on Ni(100).[9] For the last adsorbate they found the O $1s$ peak width of a $c(2\times2)$ oxygen ordered layer ranging from 1.42 eV at 150 K to 1.78 eV at 600 K, without a shift in the binding-energy position.

Here we present results on Rh{110}$(2\times2)p2mg$-O obtained at the SuperESCA beamline of Elettra.[14,15] Oxygen chemisorption on the Rh{110} surface has been extensively studied with many techniques such as high-resolution electron-energy-loss spectroscopy (HREELS),[16] low-energy electron diffraction (LEED),[17–19] scanning tunneling microscopy (STM),[20,21] helium atom scattering (HAS),[22] and XPS.[23] A variety of surface structures has been reported, depending on the coverage and temperature. Adsorption at 450 K results in a $(2\times2)p2mg$ structure at a coverage of 0.5 ML. These studies showed that at this temperature oxygen induces a $(1\times n)$ reconstruction of the rhodium substrate ($n=2-5$). In particular the LEED and HAS studies of the $(2\times2)p2mg$ structure showed that the (1×2) reconstruction present in this case is of the ''missing-row'' type, where each second close-packed $[1\bar{1}0]$ row is missing. Oxygen atoms are sitting in threefold sites in zigzag chains along the $[1\bar{1}0]$ rows. The $(2\times2)p2mg$ structure undergoes a continuous order-disorder phase transition to a (1×2) phase,[22] which falls into the two-dimensional Ising universality class. In fact, at a critical temperature T_c of 750 K the proliferation of antiphase domain walls along the [001] direction is responsible for the disorder.

In this paper we present the results of an XPS study of the O-$(2\times2)p2mg$ structure which show the effects of the anharmonicity of the potential-energy curves for the adsorbate before and after ionization (Franck-Condon principle). The O $1s$ and the O $2s$ photoemission peaks not only broaden but also shift to lower binding energy as the temperature increases. The present study contributes to the general understanding of core-level spectroscopy of atoms and molecules adsorbed on surfaces and opens a way to probe the contribution of very small effects such as anharmonic contributions in surface phenomena.

The combination of the high brightness and the high-photon energy resolution of the third generation synchrotron-radiation source, the 81-pole undulator of the SuperESCA beamline of ELETTRA, allowed us to follow the temperature variation of the surface layer every few degrees because of the short measurement time. In order to enhance the photoelectron yield the measurements were performed with a photon energy of 650 eV for the O $1s$ level and 210 eV for the O $2s$, impinging at an incidence angle of 80° from the sample surface normal. The emitted photoelectrons were collected by a VSW Class 150 multichannel electron-energy analyzer. Data collection time for a spectrum during the heating ramp was 15 and 22 sec for O $1s$ and O $2s$, respectively. The overall energy resolution, including monochromator and
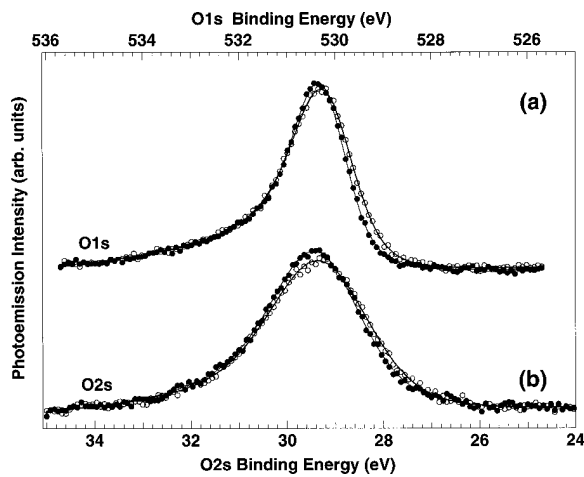
FIG. 1. Core-level O $1s$ (a) and O $2s$ (b) spectra measured at 560 K (full circles) and 810 K (open circles). The results of the fits are represented with continuous lines.

analyzer contributions, of 400 meV for the O $1s$ and 200 meV for O $2s$ levels, allowed us to distinguish small variations in the core-level line shapes. The $(2 \times 2)p2mg$ structure was obtained by dosing 0.4 L of oxygen at 570 K while looking at LEED.[23] To avoid possible loss of oxygen due to reaction with the residual gases (H_2 and CO) we left oxygen flowing during several cycles of heating up to temperatures above T_c and cooling down to room temperature checking whether the LEED intensities and full width at half maximum (FWHM) of the $(1,\frac{1}{2})$ and $(\frac{1}{2},\frac{1}{2})$ extra spots remained constant. The order of the overlayer was improved by performing several heating cycles since the formation of large islands is a thermally activated process. We performed the measurements during the heating to the maximum temperature of 870 K and also during the subsequent cooling of the sample in order to avoid possible artifacts due to extraneous effects such as desorption of the oxygen or influence of the heating current.

Figure 1 shows two of the spectra of one set, measured at 560 K (full circles) and 810 K (empty circles), for the O $1s$ (a) and the O $2s$ (b) core-level signals. The positions of the peaks clearly shift to lower binding energy and their width increases on going from low to high temperature showing a pronounced shoulder at lower binding energy.

Quantitative information on the peak shift and shape for the set of data in the range between 530–870 K was obtained by fitting the data with a Doniach-Sunjic function convolved with a Gaussian. The spectra of the clean surface were used as background. For all fits we used the line-shape parameters found for the spectra measured at lowest temperature, $T = 530$ K: a Doniach-Sunjic Lorentzian lifetime width of 0.15 eV and an asymmetry parameter of 0.18 were found to describe the measured O $1s$ spectra satisfactorily in the whole temperature range. For the O $2s$ core level the value of the Lorentzian width was 1.05 eV and the asymmetry parameter 0.1. The O $1s$ binding energy and Gaussian width after subtraction in quadrature of the instrumental resolution are illustrated in Fig. 2. In all plots, the full circles indicate the heating up set and the open circles the cooling down set.

From the plots in Fig. 2 one can see the expected linear increase of the intrinsic Gaussian width with temperature. A result is the observed temperature-induced energy position

change from 530.26 ± 0.01 eV at 560 K to 530.17 ± 0.01 eV at 870 K. To our knowledge this is the first time where a photoemission core-level peak of an adsorbate always located in the same site is observed to shift as a function of temperature. Our results are in fact different from those obtained by Nilsson and Mårtensson with O-$p(2 \times 2)$ and O-$c(2 \times 2)$ structure on Ni(100), where only a broadening of the O $1s$ peak was detected.[9]

The O $2s$ spectra, in Fig. 3, show behavior similar to that of the O $1s$ ones; the only difference is that, assuming a linear trend, the temperature slopes are steeper: ~ 0.35 meV/K compared to ~ 0.21 meV/K for the binding-energy position and ~ 0.8 meV/K against ~ 0.42 meV/K for the Gaussian peak width.
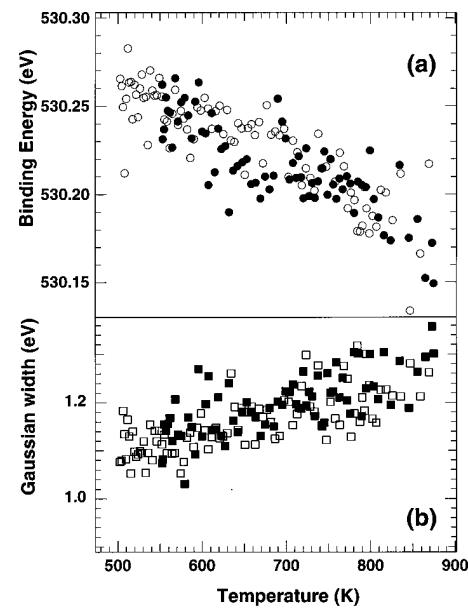

FIG. 2. O $1s$ binding energy positions (a) and FWHM (b) as a function of temperature. Full and empty symbols indicate annealing and cooling trend of the sample temperature.
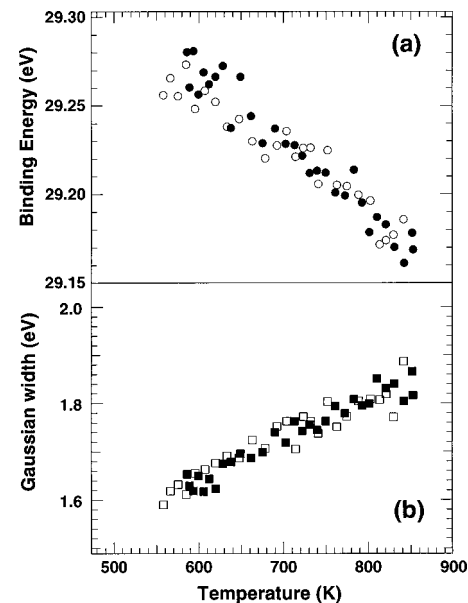

FIG. 3. O $2s$ binding-energy positions (a) and FWHM (b) as a function of temperature. Full and empty symbols indicate annealing and cooling trend of the sample temperature.

To explain the observed temperature effect we introduce the anharmonic approximation supposing a potential-energy curve asymmetric around the equilibrium bonding distance. For small compressions and extensions of the bond length from the equilibrium position ("low temperature") one can use the harmonic approximation, but for larger amplitude a more complicated behavior must be assumed.

Initial-state effects alone cannot explain the observed line shape and energy changes. Going from T_1 to T_2, the energy changes by approximately $k_B(T_1 - T_2) \sim 300 \ \mathrm{K} \times k_B \sim 25 \ \mathrm{meV}$, a value much smaller than the observed shifts. Let us consider therefore the energy difference between the initial and final state, which gives the binding-energy shift. In particular the final state can be interpreted in terms of the $Z+1$ approximation. The removal of a core electron from an atom leads essentially to the same change in the valence-electron properties as an additional positive charge added to the nucleus, i.e., the core ionized oxygen atom behaves as a fluorine atom. Fluorine is more electronegative than oxygen and is expected to adsorb at a larger distance from the surface with respect to oxygen. For these reasons we represent the initial and final state with Morse potential curves, Fig. 4, with different equilibrium bond distances. The broadening of the core-level spectrum is explained by projecting the initial-state wave function onto the final state with the occupation of different vibrational levels. The larger vibrational amplitude at elevated temperatures is manifested in the broadening of the core-level peaks towards lower binding energies. At higher temperature the asymmetric form of the potential-energy curve pushes the maximum of the vibrational-level occupation to higher bonding distances at higher temperature. In this case the energy difference between initial and final state (binding energy of the peak) decreases while going from low temperature (transition A) to high temperature (transition B).

Starting from the consideration that the ionic final state in the $Z+1$ approximation, i.e., fluorine, is placed at a larger equilibrium distance, the potential-energy curve cannot have a smaller slope at low bonding distances because this would again imply a broadening of the Gaussian contribution. On the other hand this would shift the photoemission peaks to higher binding energies, which has not been experimentally observed. The steeper slope of the potential-energy curve at shorter bonding distances with respect to the equilibrium position indicates that at higher temperature the O-Rh distance of this structure (2.05 ± 0.1 Å for this structure[19]) increases. The differences between the O $1s$ and the O $2s$ behavior is due to the fact that the $1s$ is highly localized, while the $2s$ is extended, although not as delocalized as a valence state. Therefore the two core levels sample different parts of the potential-energy well.

The importance of anharmonic contributions was already shown by other experimental techniques[24–27] for light molecules and atoms such as nitrogen and oxygen on other substrates like Ni and Cu. In the framework of the anharmonic model, we can explain the presence of a vibrational peak at 115–120 meV, observed in previous HREELS measurements[16] and originally assigned to subsurface oxygen. The existence of this peak could be attributed to overtones, which are observed at a frequency slightly lower than
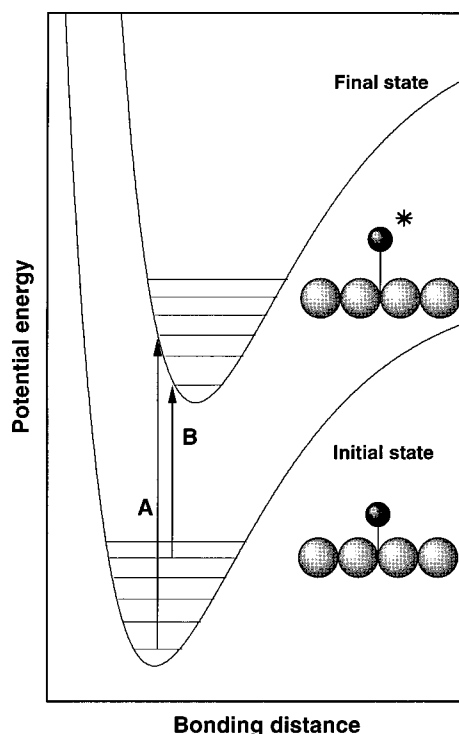

FIG. 4. Anharmonic potential representation of the initial- (neutral) and final-state (ionized) potential-energy curves. Low- and high-temperature transitions have been indicated by A and B, respectively.

a multiple of the fundamental frequency (65 meV), and interpreted due to the anharmonic behavior of the potential-energy curve.

We can exclude as a cause of the energy shift the order-disorder phase transition taking place at 750 K,[22] because one should expect in this case a discontinuous broadening of the core-level peaks at the critical temperature. The proliferation of antiphase domain walls along the [001] direction on approaching the critical temperature, maintains the first nearest-neighbor distance constant while changing slightly the distances along the [$1\bar{1}0$] directions, which corresponds to twice the distance of the rhodium (100) units cell in the same direction. This distance is large and we believe that the interaction changes are negligible and cannot affect the core-level binding energies. Instead, effects due to order-disorder transitions have been revealed with vibrational techniques resulting in discontinuous changes in the FWHM of the infrared absorption spectroscopy peaks.[28,29]

Although quantitative understanding of the observed phenomena is not easy to achieve, our data clearly demonstrate the utility of the photoemission approach for studying the potential-energy well of adsorbates. Advanced *ab initio* theoretical calculations which take into account initial- and final-state contribution in the photoemission process and comparison with the experimental results are therefore necessary to reach a general understanding of the phenomena.

[1] D. Menzel, Surf. Sci. **299/300**, 170 (1994).

[2] A. Nilsson and N. Mårtensson, J. Electron Spectrosc. Relat. Phenom. **75**, 209 (1995).

[3] D. M. Riffe, G. K. Wertheim, D. N. E. Buchanan, and P. H. Citrin, Phys. Rev. B **45**, 6216 (1992).

[4] G. K. Wertheim, P. H. Citrin, and J. F. Van der Veen, Phys. Rev. B **30**, 4343 (1984).

[5] G. K. Wertheim, D. M. Riffe, and P. H. Citrin, Phys. Rev. B **49**, 2277 (1994).

[6] D. M. Riffe, G. K. Wertheim, and P. H. Citrin, Phys. Rev. Lett. **67**, 116 (1991).

[7] W. Theis and K. Horn, Phys. Rev. B **51**, 7157 (1995).

[8] J. W. Gadzuk, S. Holloway, C. Mariani, and K. Horn, Phys. Rev. Lett. **48**, 1288 (1982).

[9] A. Nilsson and N. Mårtensson, Phys. Rev. Lett. **63**, 1483 (1989).

[10] A. Nilsson and N. Mårtensson, Solid State Commun. **70**, 923 (1989).

[11] N. Mårtensson and A. Nilsson, J. Electron Spectrosc. Relat. Phenom. **52**, 1 (1990).

[12] N. Mårtensson and A. Nilsson, Surf. Sci. **211**, 303 (1989).

[13] H. Antonsson, N. Mårtensson, and A. Nilsson, J. Electron Spectrosc. Relat. Phenom. **54/55**, 601 (1990).

[14] A. Abrami *et al.*, Rev. Sci. Instrum. **66**, 1618 (1995).

[15] A. Baraldi, M. Barnaba, B. Brena, D. Cocco, G. Comelli, S. Lizzit, G. Paolucci, and R. Rosei, J. Electron Spectrosc. Relat. Phenom. **67**, 211 (1994).

[16] D. Alfè, P. Rudolf, M. Kiskinova, and R. Rosei, Chem. Phys. Lett. **211**, 220 (1993).

[17] M. Gierer, H. Over, G. Ertl, H. Wohlgemuth, E. Schwarz, and K. Christmann, Surf. Sci. **297**, L73 (1993).

[18] J. D. Batteas, A. Barbieri, E. K. Starkey, M. A. Van Hove, and G. A. Somorjai, Surf. Sci. **339**, 142 (1995).

[19] C. Comicioli, V. R. Dhanak, G. Comelli, C. Astaldi, K. C. Prince, A. Atrei, and E. Zanazzi, Chem. Phys. Lett. **214**, 438 (1993).

[20] V. R. Dhanak, K. C. Prince, R. Rosei, P. W. Murray, F. M. Leibsle, M. Bowker, and G. Thornton, Phys. Rev. B **49**, 5585 (1994).

[21] P. W. Murray, F. M. Leibsle, Y. Li, Q. Guo, M. Bowker, G. Thornton, V. R. Dhanak, K. C. Prince, and R. Rosei, Phys. Rev. B **47**, 12 976 (1993).

[22] A. F. Bellman, D. Cvetko, A. Morgante, M. Polli, F. Tommasini, K. C. Prince, and R. Rosei, Surf. Sci. Lett. **281**, L321 (1993).

[23] G. Comelli, A. Baraldi, S. Lizzit, D. Cocco, G. Paolucci, M. Kiskinova, and R. Rosei, Chem. Phys. Lett. **261**, 253 (1996).

[24] D. Arvanitis and K. Baberschke, J. Electron Spectrosc. Relat. Phenom. **75**, 149 (1995).

[25] F. Sette, T. Hashizume, F. Comin, A. A. MacDowell, and P. H. Citrin, Phys. Rev. Lett. **61**, 1384 (1988).

[26] L. Wang and D. Shirley (private communication).

[27] L. Wenzel, D. Arvanitis, H. Rabus, T. Ledere, K. Baberschke, and G. Comelli, Phys. Rev. Lett. **64**, 1765 (1990).

[28] R. Ryberg, Phys. Rev. B **40**, 865 (1989).

[29] R. Ryberg, Phys. Rev. B **40**, 8567 (1989).